Vertebral level specific modulation of paraspinal muscle activity based on vestibular signals during walking.

Yiyuan C. Li,[1,2] Sjoerd M. Bruijn,[1] Koen K. Lemaire[1], Simon Brumagne[2], Jaap H. van Dieën [1]
[1]Department of Human Movement Sciences, Faculty of Behavioral and Movement Sciences, Vrije Universiteit Amsterdam, Amsterdam Movement Sciences, Amsterdam, The Netherlands
[2] Department of Rehabilitation Sciences, KU Leuven, Leuven, Belgium

Correspondence: Jaap H. van Dieën (j.van.dieen@vu.nl)

Abstract

Evoking muscle responses by electrical vestibular stimulation (EVS) may help to understand the contribution of the vestibular system to postural control. Although paraspinal muscles play a role in postural stability, the vestibulo-muscular coupling of these muscles during walking has rarely been studied. This study aimed to investigate how vestibular signals affect paraspinal muscle activity at different vertebral levels during walking with preferred and narrow step width. Sixteen healthy participants were recruited. Participants walked on a treadmill for 8 minutes at 78 steps/min and 2.8 km/h, at two different step width, either with or without EVS. Bipolar electromyography was recorded bilaterally from the paraspinal muscles at eight vertebral levels from cervical to lumbar. Coherence, gain, and delay of EVS and EMG responses were determined. Significant EVS-EMG coupling ($p<0.01$) was found at ipsilateral and/or contralateral heel strikes. This coupling was mirrored between left and right relative to the midline of the trunk and between the higher and lower vertebral levels, i.e., a peak occurred at ipsilateral heel strike at lower levels, whereas it occurred at contralateral heel strike at higher levels. EVS-EMG coupling only partially coincided with peak muscle activity. EVS-EMG coherence slightly, but not significantly, increased when walking with narrow steps. No significant differences were found in gain and phase between the vertebral levels or step width conditions. In summary, vertebral level specific modulation of paraspinal muscle activity based on vestibular signals might allow a fast, synchronized, and spatially co-ordinated response along the trunk during walking.

Keywords: electrical vestibular stimulation, paraspinal muscles, balance control, gait stability

Introduction

Stable walking, defined as “gait that does not lead to falls” (Bruijn *et al.*, 2013), is an effortless and seemingly simple task for healthy young adults. However, with the presence of disorder (e.g., low back pain, bilateral vestibular loss, etc.), aging, or external perturbations, the difficulty of the task becomes manifest (Mazaheri *et al.*, 2013; Sprenger *et al.*, 2017). To maintain stability, the centre of mass should be controlled relative to the base of support. Three mechanisms can contribute to the control of the centre of mass: modulation of foot placement, shifting the centre of pressure through ankle moments, and changing angular momentum such as through trunk rotation (known as counter-rotation) (Hof, 2007).

These mechanisms for stability are believed to be controlled using the error between efference copies and the actual state detected by sensory systems. The vestibular system, for instance, which encodes head motion, has been shown to contribute to gait stabilization (van Schooten *et al.*, 2011; Cullen, 2012; Magnani *et al.*, 2021). It has been reported that the medial vestibulospinal tract, commencing in the medial vestibular nucleus and then bilaterally extending through the cervical spinal cord into the medial longitudinal fasciculus, is involved in head stabilization (Wilson & Maeda, 1974; Fukushima *et al.*, 1979; Goldberg & Cullen, 2011; Forbes *et al.*, 2020). Another descending brainstem pathway involved in stabilization is the lateral vestibulospinal tract, which originates in the lateral vestibular nucleus and projects ipsilaterally to axial motoneurons at all spinal levels (Grillner & Hongo, 1972; Fukushima *et al.*, 1979; Basaldella *et al.*, 2015). This pathway is required for the preservation of upright posture and for responding to postural perturbations (Markham, 1987; Dichgans & Diener, 1989; Murray *et al.*, 2018). The vestibulospinal reflex has been investigated experimentally by applying electrical vestibular stimulation (EVS). This stimulation activates the vestibular afferent nerve fibres without head movements and produces an illusion of moving the head (Goldberg *et al.*, 1982; Day, 1999; Kwan *et al.*, 2019). Consequently, muscle responses can be detected in balance related muscles while standing and walking (Ali *et al.*, 2003; Dakin *et al.*, 2010; Guillaud *et al.*, 2020; Magnani *et al.*, 2021). Studies have revealed that these muscle responses are frequency, task, and muscle specific (Dakin *et al.*, 2010; Forbes *et al.*, 2013).

While the responses of lower limb muscles to vestibular stimulation during walking have been extensively investigated (Forbes *et al.*, 2013; Magnani *et al.*, 2021), little attention has been given to the trunk muscle responses to EVS, despite the fact that the upper body represents approximately 50% of the total body mass (de Leva, 1996). In the study of gait, most attention has been devoted to the control of the legs, whereas body parts above the hips are commonly considered as a single rigid head-arm-trunk segment. However, in terms of maintaining stability, the trunk may play a significant role, as even a tiny deviation from the perfect upright position can produce a substantial destabilizing moment (Bruijn & van Dieen, 2018). Additionally, the trunk may be crucial when employing the counter-rotation mechanism for stabilization (Hof, 2007).

A narrow step width, which reduces the base of support, poses greater challenges to stability and, as such, increases the demands on postural control (Arvin *et al.*, 2016; Magnani *et al.*, 2023). A previous study demonstrated that vestibular contributions

are modulated by the stabilization demands of walking (Magnani *et al.*, 2021). This study showed an increased coherence between EVS and ground reaction force during walking with narrow steps but decreased EVS-ground reaction force coherence during walking with wider steps. Though the coherence between EVS and EMG of lower limb muscles remained unchanged or decreased, the EVS-EMG coherence increased in the paraspinal muscles at the lumbar region when walking with a narrow step width (Magnani *et al.*, 2021). Overall, these findings indicate the importance of coupling between vestibular signals and paraspinal muscles in controlling stability during walking. However, while this previous study did look at the paraspinal muscles, it only studied the paraspinal muscles at one vertebral level of the trunk. It is therefore unknown if, and how, paraspinal muscles at other vertebral levels are involved in the control of gait stability.

Our research question was: If and how do paraspinal muscles at different vertebral levels respond to electrical vestibular stimulation throughout the gait cycle? Furthermore, we tested if these vestibular contributions varied with step width. Based on previous studies (Forbes *et al.*, 2013; Magnani *et al.*, 2021), we hypothesized that: 1) paraspinal muscle show activity coherent with EVS at specific phases of the gait cycle, specifically at heel strike; 2) the EVS-evoked muscles responses increase when walking with narrow step widths. To test our hypotheses, we characterized the coherence, gain and delay of EMG-electrical vestibular stimulation response in paraspinal muscle during walking with both preferred step width and narrow step width. Paraspinal muscles from cervical to lumbar vertebral levels were studied.

Methods

Participants

Sixteen healthy participants (7 male, 9 female) between the ages of 19 and 29 years were recruited (Age: 23.5 ± 3.4 years, height: 1.71 ± 0.07 m, weight: 64.5 ± 13.2 kg). Exclusion criteria for participation included any diagnosed orthopaedic or neurological disorders, or the use of medications that can cause dizziness. Participants were instructed not to engage in intense physical exercise and to refrain from alcohol consumption 24 hours prior to the experiment. Two participants were excluded during data analysis due to technical problems in the signal synchronization between devices. The participants agreed to participate in the study by signing an informed consent form. Procedures conformed to relevant guidelines and regulations and had been approved by the VU Amsterdam Research Ethics Committee VCWE-2022-126.

Electrical Vestibular Stimulation

Continuous EVS was applied in a bipolar configuration. The EVS was delivered as an analogue signal via a digital-to-analogue converter (National Instruments Corp., Austin, USA) to an isolated constant-current stimulator (BIOPAC System Inc., Goleta, USA) that was connected to carbon rubber electrodes (9cm²). The two electrodes were coated with electrode gel (SonoGel, Bad Camberg, Germany) and placed over the mastoid processes, fixed tightly with hypoallergenic tapes and an elastic head band.

All the participants were exposed to the same zero-mean stochastic EVS signal, which was a white noise generated in Matlab (2019a, The MathWorks, Natick, US) with a bandwidth from 0 to 25Hz, peak amplitude of ± 5.0 mA, and duration of 8 minutes. These signal characteristics were identical to those used previously (Magnani *et al.*, 2021).

Electromyography and Ground Reaction Force Measurement

Bipolar surface electromyography (EMG) was recorded by the 64-channel REFA amplifier (TMSi, Oldenzaal, The Netherlands; CMRR: > 90 dB; Input impedance: > 100 MΩ; Gain: 26.55), bilaterally from the paraspinal muscles at 2048 samples/s using disposable self-adhesive Ag/AgCl surface electrodes (Ambu blue sensor, Ballerup, Denmark). EMG was recorded from paraspinal muscles at eight vertebral levels, including the seventh cervical vertebra (C7), the third, fifth, seventh, nineth and twelfth thoracic vertebra (T3, T5, T7, T9, T12) and the second and fourth lumbar vertebra (L2, L4). After shaving, lightly abrading, and cleaning the skin with alcohol, electrodes were placed 2 to 3 cm lateral to the mid-sagittal line, defined by the spinous processes (Figure 1). A reference electrode was placed over the bony part of the acromion process.

Ground reaction forces (GRF) were measured at a sampling rate of 1000 Hz by force plates, which were built-in the split-belt treadmill (ForceLink b.v., Culemborg, the Netherlands). The force plate data were used to identify heel-strike. Kinematic data were recorded using a 3D motion capture system (Northern Digital Inc, Waterloo Ont, Canada), sampling at 50 samples/s, to calculate the step widths.

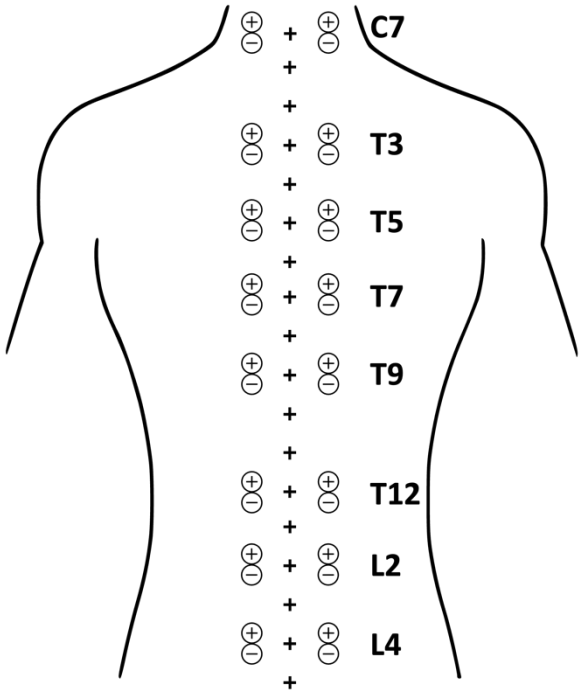

Figure 1. EMG Electrodes Placement.
The locations of the paired electrodes over the paraspinal muscles at eight vertebral levels from top to bottom: C7, T3, T5, T7, T9, T12, L2 and L4. Electrodes were placed 2 to 3 cm lateral to the mid-sagittal line defined by the spinous processes, which are indicated by the plus symbols ('+').

Protocol
Prior to the start of the experiment, participants were asked to walk on the dual-belt treadmill at a speed of 2.8 km/h without EVS for 3 minutes to measure their preferred step widths (PSW). For familiarization, participants were exposed to vestibular stimulation in a three-minutes-walk at 2.8 km/h. In addition, they were instructed to time their steps to the beat of a metronome at 78 steps/min.

For the experiment, participants walked on the dual-belt treadmill at 2.8 km/h with a cadence of 78 steps/min for 8 minutes. Walking speed and cadence were chosen to replicate the conditions of Magnani et al. (2021). The conditions were defined by the presence of EVS (EVS and no-EVS), by the step width (preferred step width: PSW and narrow step width: NSW) and by head orientation (facing forward and facing sideways). Participants were instructed to face forward in all conditions except in head sideways condition. Data from head sideways condition were not used in this study. NSW was defined as 50% of PSW. To impose step width, two lines were projected on the treadmill, symmetrical to its midline. Participants were instructed to align the middle of their shoes with these lines and to check the line with peripheral vision (Arvin et al., 2016). The order of the conditions was randomized for each participant. Throughout the trials, participants received repeated verbal instruction to maintain their cadence and step width. Before each trial, participants were given

sufficient time to rest, followed by 2 min walking without vestibular stimulation before data collection, to avoid acclimatization and/or habituation effects.

Signal Analysis

The electromyography, force plate and vestibular stimulation signals were first synchronized based on the trigger signals. Subsequently, EMG signals (2048 Hz) were resampled to 1000 Hz, aligned with the sampling rate of the force plate and EVS signals. Time instances of heel strikes were calculated from force plate data from the characteristic "butterfly pattern" of the centre of pressure (Roerdink et al., 2008). To test if, and how well participants were able to execute the task of controlling step widths and cadence, the mean step width of each participant was calculated as the mediolateral distance between the second toe tip markers during heel strikes. The cadence was calculated from the time between subsequent heel strikes of the same leg.

The vestibular stimulation caused artifacts in the EMG signals, particularly when recording from the cervical and upper thoracic region (Ali *et al.*, 2003). To avoid the artifacts, the bipolar EMG signals were high pass filtered with a 6th order, Butterworth high pass filter with a cut-off frequency of 100 Hz (Forbes *et al.*, 2013), rectified, and normalized to the maximum amplitude of EMG from the averaged gait cycle in the No-EVS-PSW condition for each vertebral level and participant.

Estimates of coherence, gain and phase were based on the continuous Morlet wavelet decomposition (Blouin *et al.*, 2011). Before calculating the auto- and cross-spectra, EVS and normalized EMG signals were first sectioned into strides based on the right heel strikes. To avoid distortion in the coherence and gain calculation at either the beginning or the end of the signals, each stride was padded with data from the previous (50%) and subsequent (50%) strides. Time-frequency coherence, $Coh(\tau, f)$, was computed to measure the linear relationship between the EVS and EMG signals across the frequencies considered as:

$$Coh(\tau, f) = \frac{\left|CSD_{xy}(\tau, f)\right|^2}{PSD_{xx}(\tau, f)\, PSD_{yy}(\tau, f)}$$

Where τ and f denote the stride time and frequency, $CSD_{xy}(\tau, f)$ refers to the time-frequency cross-spectra between EVS and normalized EMG. $PSD_{xx}(\tau, f)$ and $PSD_{yy}(\tau, f)$ are the time-frequency auto-spectra of EVS and EMG, respectively. To account for the variability of stride duration, time was normalized by resampling the CSD_{xy}, $PSD_{xx}(\tau, f)$ and $PSD_{yy}(\tau, f)$ to 1000 samples per stride cycle. Coherence, which is unitless, ranges from 0 to 1, with 0 indicating independence and 1 indicating a perfect linear relationship between the two signals. Under the hypothesis that the stimulation signal and output signal are independent, the distribution of coherence estimate can be written as (Zhan *et al.*, 2006):

$$P(R^2 \leq r) = 1 - (1 - r)^{K-1}, 0 \leq r \leq 1$$

where $P(R^2 \leq r)$ denotes the probability of coherence (R^2) less than the detection threshold (r) and K is the number of strides for each participant. For a 99% confidence interval, corresponding to $p < 0.01$, the threshold of coherence estimate is

0.015 with K as 300 strides, which was the minimum number of strides across all subjects.

To unveil the magnitude and timing of the output EMG relative to the input EVS, gain and phase estimates were calculated from the frequency response function (FRF), defined as:

$$FRF(\tau, f) = \frac{CSD_{xy}(\tau, f)}{PSD_{xx}(\tau, f)}$$

Where $FRF(\tau, f)$ indicates the time-frequency frequency response function. The FRF is a complex function, the modulus of which represents the gain (1/milliampere, mA^{-1}), and the angle indicates the phase estimate (radian, rad). Since the gain and phase are not interpretable when the coherence between input and output is weak, we only used the phase and gain where the coherence reached its peak. The peak time-frequency coherence was defined as follows: first, the non-significant coherence estimates were removed for each participant and each vertebral level. The peak coherence was defined as the range of frequencies and gait phases where the coherence was larger than 99% of the remaining (significant) coherence estimates. Time-frequency phase estimates were then exacted from the region of peak coherence and transformed into time lags (millisecond, ms). Subsequently, the gain and delay were defined as the median of the gains and time lags across the frequencies and gait phases at peak coherence for each vertebral level and each participant. Gain and delay estimates from the left and right recording sites at the same vertebral level were averaged.

Statistical Analysis

The assumption of normality was checked via the Shapiro-Wilk test ($p > 0.05$). Subsequently, a paired samples t-test and a paired samples Wilcoxon test were performed respectively to compare step widths and cadences between step width conditions, respectively. As the coherence ranges from 0 to 1, the modified Fisher-Z transform was applied on coherence before statistical analysis. For each participant, coherence exceeding 0.015, (i.e., $p < 0.01$), was defined as significant. To identify whether the paraspinal muscle responses significantly differed between step widths, we performed cluster-based permutation tests (paired t-tests, 2000 permutations) on coherence (Maris et al., 2007). To test the differences in delays and gains, repeated-measures analysis of variance (ANOVAs) with two factors: Vertebral level (eight vertebral levels) × Condition (preferred step width and narrow step width) were performed. The assumption of sphericity for repeated-measures ANOVAs was verified by Mauchly's Test ($p > 0.05$). Greenhouse-Geisser correction was applied when the assumption of sphericity was rejected. Significance was set at $p < 0.05$ for the statistical tests. Statistical analyses were performed in MATLAB (2019a, The MathWorks, Natick, US).

Results

Although step width during walking with narrow step widths was not halved when compared to walking with preferred step width, it was significantly smaller than during walking with preferred step width (t (13) = 9.56, $p < 0.001$) (Figure 2A). In both conditions, the cadence (Figure 2B) was higher than instructed (78 steps/min), but it was not significantly different between conditions (W (13) = -19, $p = 0.58$).

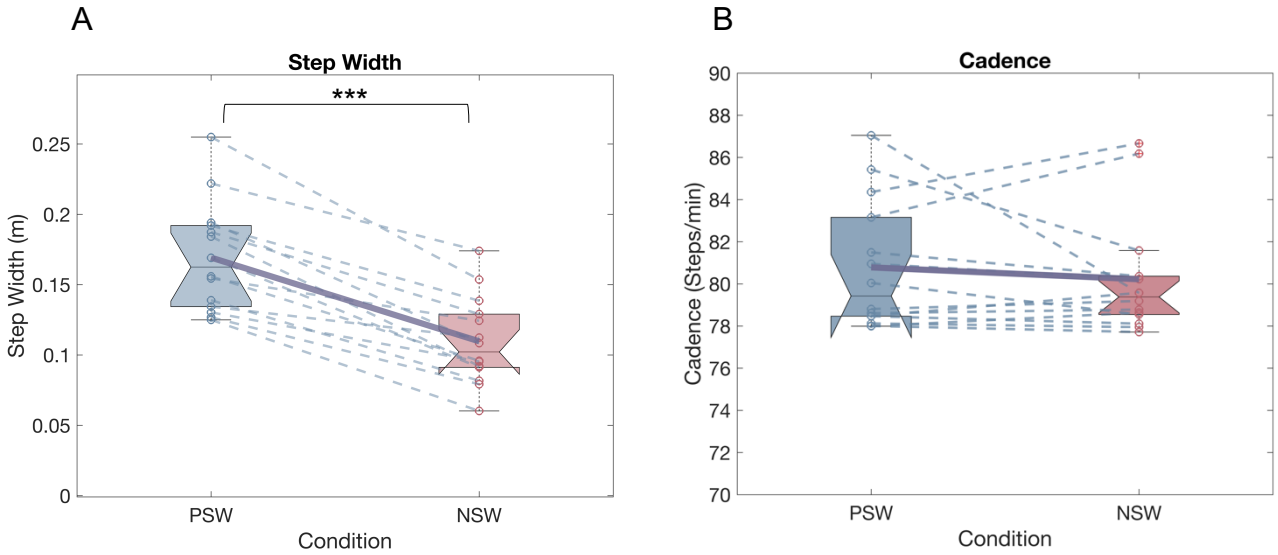

Figure 2. (A) Step Width and (B) Cadence in Two Step Width Conditions. Thick lines represent the mean values, while the thin lines depict individual data. Within each box, the centre mark indicates the median, and the bottom and top edges indicate the 25th and 75th percentiles, respectively. The whiskers extend to the maximum and minimum values, excluding the outliers. Significance is denoted by *** ($p < 0.001$).

Paraspinal Muscles Activity During Walking in Two Step Widths Conditions
No significant differences were induced by the presence of EVS in muscle activity in either magnitude or the pattern of muscle activity (Supplementary material 1).

Normalized muscle activity recorded from the paraspinal muscles at eight vertebral levels (C7, T3, T5, T7, T9, T12, L2, L4, bilaterally) during walking with electrical vestibular stimulation (EVS) with preferred step widths (PSW) and narrow step widths (NSW) is illustrated in Figure 3. All recorded sites exhibited rhythmic modulation over the gait cycle, but the modulation appeared more pronounced for the lower vertebral levels.

There were few to no differences in averaged muscle activity between walking with preferred and narrow step widths, except at ipsilateral heel strike at C7L ($p = 0.018$) and L2L ($p = 0.019$), where the muscle activity was significantly higher when walking with narrow step widths (Supplementary material 2). At higher vertebral levels, including C7, T3, T5, T7 and T9, peaks occurred just after the contralateral heel strikes. At lower vertebral levels (T12, L2 and L4), muscle activity demonstrated two peaks occurring just after both ipsilateral and contralateral heel strikes.

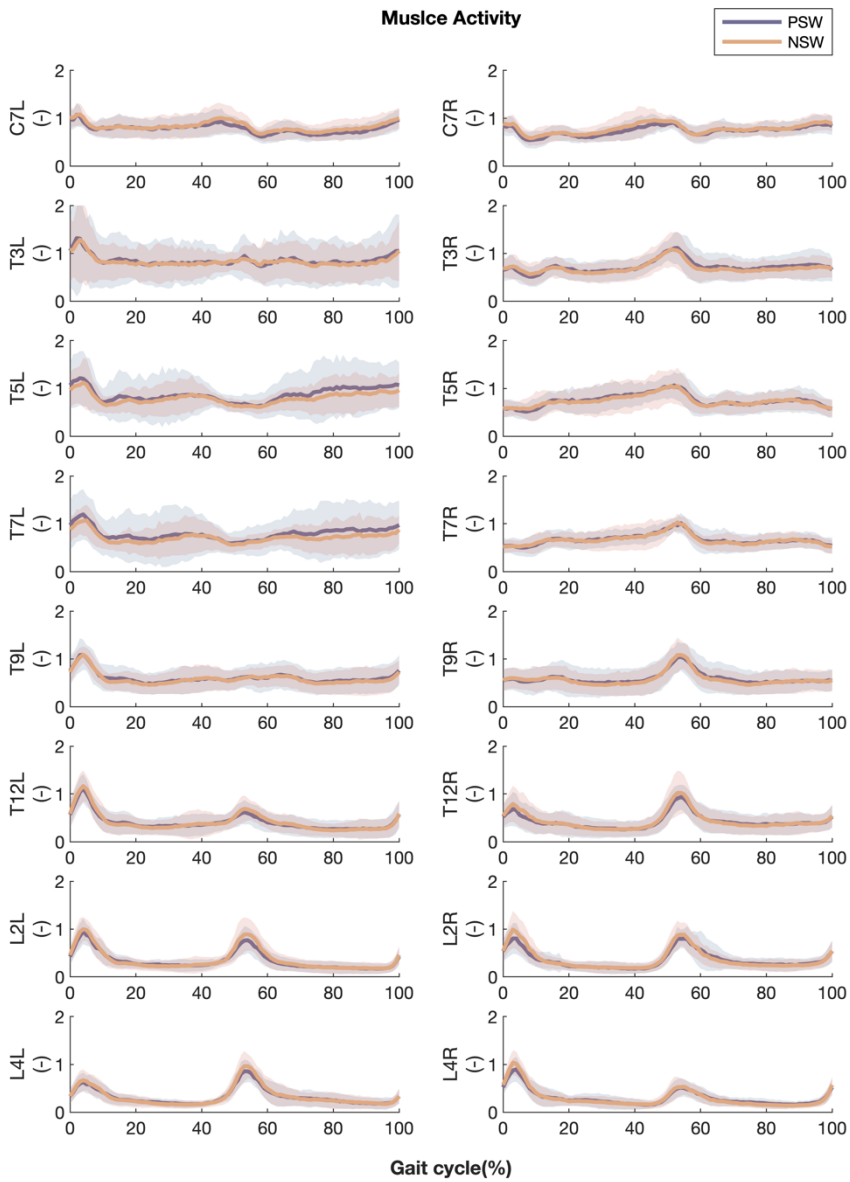

Figure 3. Paraspinal Muscle Activity Throughout the Gait Cycle.
Averaged EMG linear envelopes of paraspinal muscles at all investigated vertebral levels during walking with EVS at preferred step width (Blue) and narrow step width (Red). The X-axis indicates the time (normalized to gait cycle, starting at the right heel strike). The Y-axis presents the amplitude of the normalized EMG. The lines and shadowed areas represent the means and standard deviations across participants, respectively. The left and right columns depict recorded sites at the left and right side relative to the midline of the trunk. From top to bottom rows, the EMG of paraspinal muscles at eight vertebral levels are displayed as: C7, T3, T5, T7, T9, T12, L2 and L4.

EVS-EMG Coherence During Walking with Preferred Step Width
Significant EVS-EMG coupling, defined as coherence over 0.015, was observed in all recorded sites when walking with preferred step width. But differences between vertebral levels as to when, and in which frequency band this coherence occurred were found (Figure 4).

Phase-specific EVS-EMG coherence was roughly mirrored in the left and right relative to the midline of trunk, i.e., phase shifted by about half a gait cycle. Cluster-based permutation paired t-test showed no significant differences between coherence at left and right when they were shifted by half a gait cycle (Supplementary material 3).

At vertebral levels from T12 to L4, peak coherence occurred around the ipsilateral heel strikes. At T7 and T9, peak coherence occurred before both ipsilateral and contralateral heel strikes. At vertebral levels from T3 to T5, peak coherence occurred around the contralateral heel strikes. At C7 level, coupling between EVS and EMG was almost continuously present, without distinct peaks, albeit at an overall lower magnitude. Overall, the phase-specific responses at the higher and lower vertebral levels were also mirrored, such that at lower levels a peak occurred at ipsilateral heel strike, while at higher levels, it occurred at contralateral heel strike.

Additionally, responses occurred earlier in the gait cycle at the higher vertebral levels compared to the lower levels. The magnitude of coherence was higher at the lower vertebral levels. Peak coherence aligned with one of the peaks in muscle activity at the lower vertebral levels (i.e., ipsilateral heel strike), and with the only peak, at contralateral heel strikes, for the higher vertebral levels.

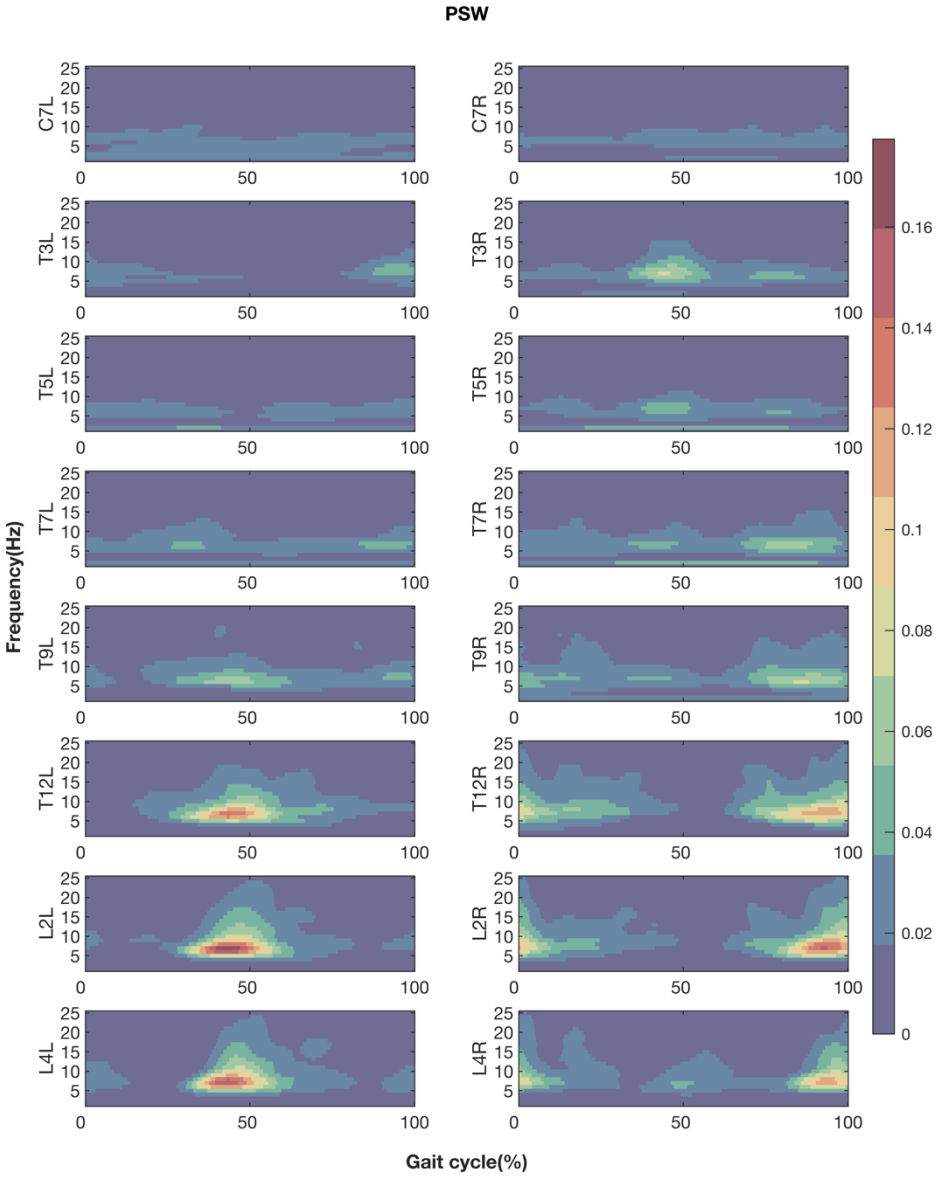

Figure 4. EVS-EMG Coherence Throughout the Gait Cycle During Walking with Preferred Step Width.
Coherence between EVS and EMG of paraspinal muscles at C7, T3, T5, T7, T9, T12, L2 and L4 levels (from top to bottom) during walking with preferred step widths while exposed to EVS. The left and right columns represent the recorded sites at the left and right side relative to the mid-line of the trunk. The X-axis is the time (normalized to gait cycle, starting at the right heel strike). The Y-axis is the frequency range (from 1Hz to 25 Hz). Coherence amplitude is indicated by the colour bar. For illustrative purposes, only coherence above 0.015 are presented.

EVS-EMG Coherence During Walking with Narrow Step Width

To address our hypothesis that the magnitude of coupling between EVS and EMG during walking with narrow step width is larger than walking with preferred step width, the differences in EVS-EMG coherence between walking with preferred step width (PSW) and walking with narrow step width (NSW) were examined (Figure 5B).

At the majority of vertebral levels, during most of the phases in the gait cycle, EVS-EMG coupling during walking with a narrow step width was slightly, but not significantly, higher than that during walking with preferred step width (Figure 5A). The greatest differences were observed at the instants around the peak coherence in normal walking. Interestingly, at the L4 level on both sides, there was a decrease in coherence when walking with a narrow step width, around the contralateral heel strikes, but again this was not significant.

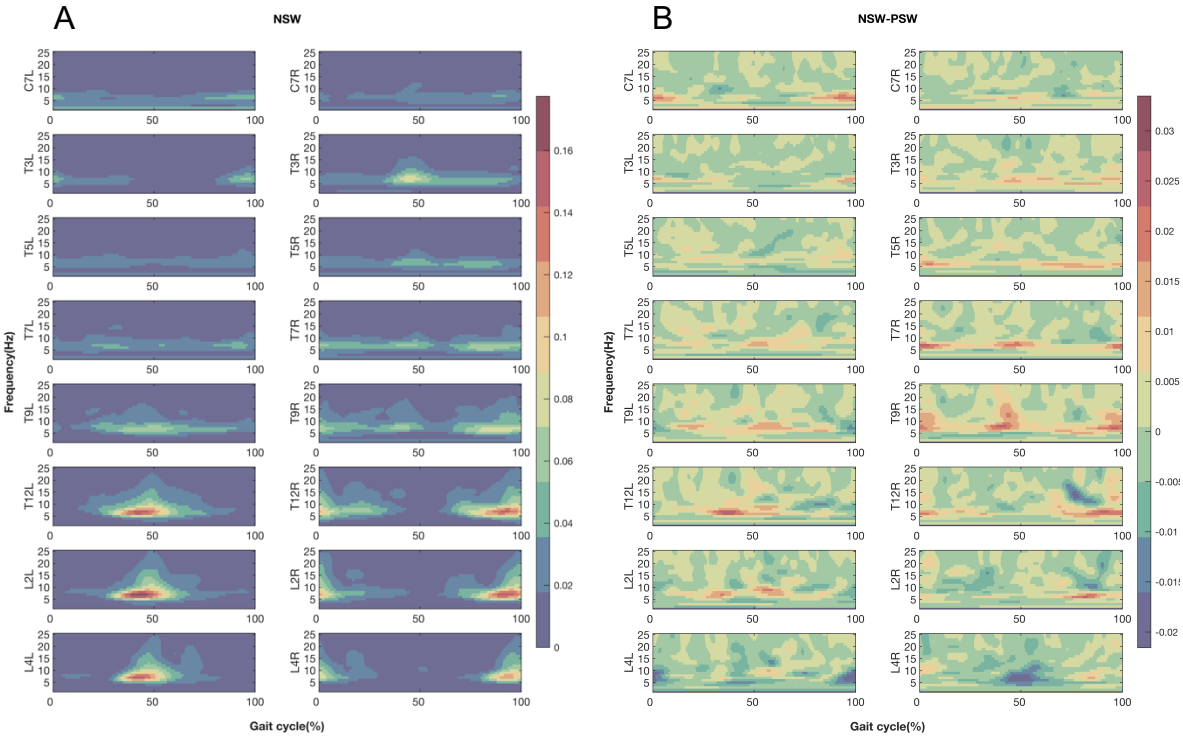

Figure 5. EVS-EMG Coherence in NSW and Effects of Step Width.
(A) The coherence between EVS and EMG when walking with narrow step width (NSW); (B) The difference in coherence between walking with narrow step widths and preferred step width (NSW - PSW). Figures from top to bottom rows present the results at eight vertebral levels. The left or right columns represent the recorded sites at the left or right side relative to the mid-sagittal line of trunk. The X-axis is the time (normalized to gait cycle, starting at the right heel strike). The Y-axis is the frequency range (from 1Hz to 25 Hz). The magnitudes of coherence in NSW (A) and the difference of coherence between NSW and PSW (B) are indicated by the colour bar.

Gain and Delay Estimates Between EVS and EMG

No significant effects on gains of either Vertebral level ($F(7, 30.43) = 1.64$, $p = 0.20$), Condition ($F(1, 4.35) = 0.74$, $p = 0.39$), or their interaction ($F(7, 30.43) = 1.73$, $p = 0.15$) were found (Figure 6A).

After Greenhouse-Geisser correction, no significant effects on delays of Vertebral level ($F(7, 65.21) = 2.18$, $p = 0.09$), Condition ($F(1, 9.32) = 1.16$, $p = 0.29$), or Vertebral level x Condition interaction ($F(7, 65.21) = 1.64$, $p = 0.18$) were found (Figure 6B).

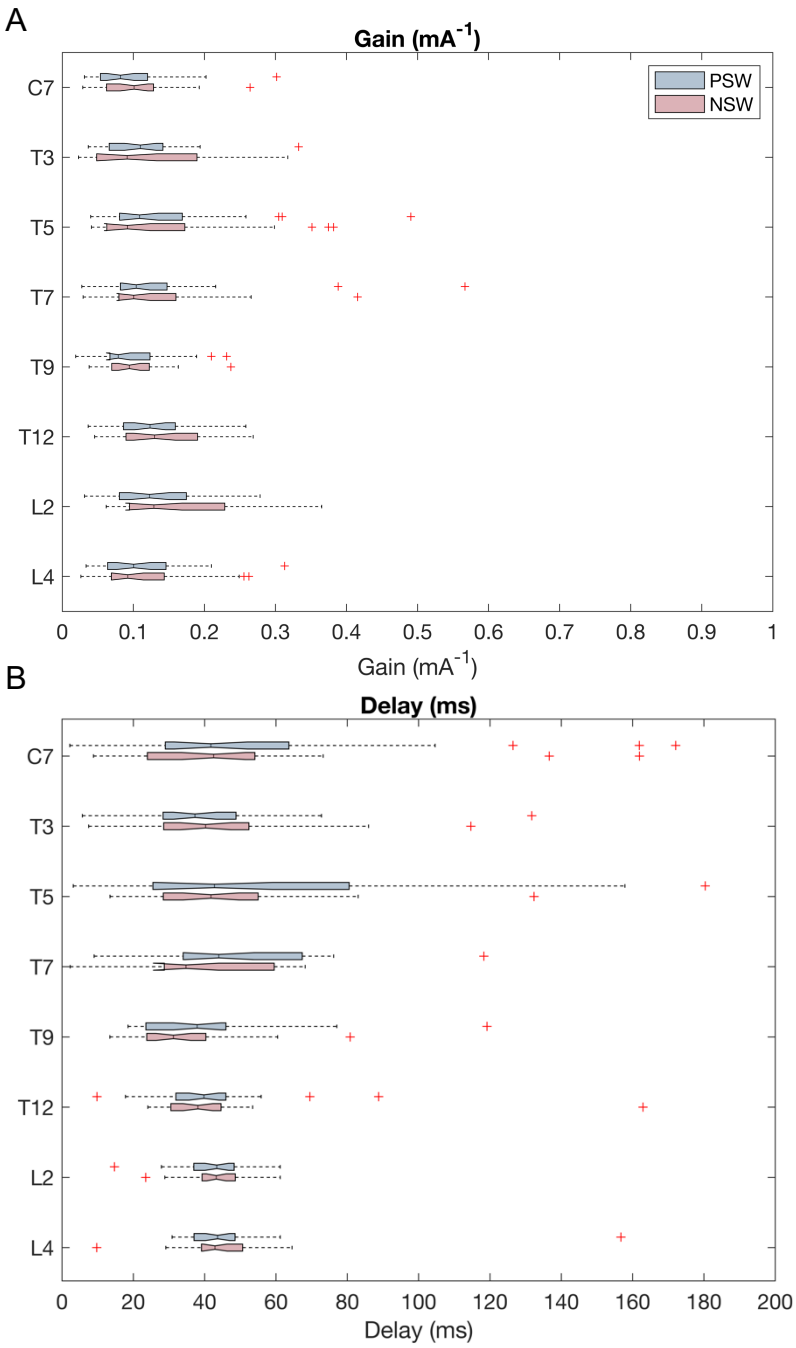

Figure 6. Gain and Delay Estimates Between EVS and EMG
The Y-axis represents vertebral levels (C7, T3, T5, T7, T9, T12, L2 and L4). In panel A, the X-axis represents the magnitude of the gain (mA^{-1}) between EVS and EMG during walking with preferred (red box) and narrow step widths (blue box). In Panel B, the X-axis represents the delay (ms) between EVS and EMG. Within each box, the central mark indicates the median, and the bottom and top edges indicate the 25th and 75th percentiles, respectively. The red '+' symbols represent the outliers, and the whiskers extend to the maximum and minimum values, excluding the outliers.

Discussion

We used electrical vestibular stimulation (EVS) and EMG to investigate the coupling of vestibular afference to paraspinal muscles activity at different vertebral levels. No significant differences were induced by the presence of EVS in muscle activity in either magnitude or the pattern of activity. Significant coherence between the input EVS signal and output paraspinal muscle EMG, from cervical to lumbar vertebral levels, was found at ipsilateral and/or contralateral heel strikes. This coupling between EVS and EMG was roughly mirrored between the left and right body sides, i.e., phase shifted about half a gait cycle. Between the higher and lower vertebral levels, the coupling was also mirrored, such that a peak coherence occurred at ipsilateral heel strike at lower vertebral levels, while at higher levels it occurred at contralateral heel strike. EVS-EMG coupling only partially coincided with the peak muscle activity. Small but non-significant increases were found in EVS-EMG coupling during walking with narrow step widths. Below, we discuss how these findings advance our understanding of the contribution of the vestibular system to the control of paraspinal muscles.

The Contribution of The Vestibular System to Paraspinal Muscle Activity
No significant differences were induced by the presence of EVS in muscle activity in either magnitude or the pattern of activity. Similar to previous studies, paraspinal muscles showed peak activity around both heel strikes at the lower vertebral levels (Ivanenko *et al.*, 2004; de Seze *et al.*, 2008; Guillaud *et al.*, 2020; Magnani *et al.*, 2021) and only a single peak at contralateral heel strikes at the higher vertebral levels (Ivanenko *et al.*, 2006). However, at the higher spinal levels, de Seze et al (2008) reported a double-peaked pattern with a relatively smaller magnitude at ipsilateral heel strike. The difference in peak muscle activity at higher vertebral levels could be attributed to the lower walking speed in our study (2.8 km/h) as compared to the study of de Seze et al (2008) at 5 km/h, since the trunk muscle activity increases with walking speed (Callaghan *et al.*, 1999; Anders *et al.*, 2007).

At the higher vertebral levels, we found the EVS-EMG coupling partially aligned with the only peak in EMG in the gait cycle at contralateral heel strike. At the lower vertebral levels, we found that the peak EVS-EMG coupling partially aligned with the peak muscle activity at ipsilateral heel strike. At the contralateral heel strike, no significant EVS-EMG coupling was observed, in spite of the peak in muscle activity. This indicates that high motoneuron excitability does not necessarily cause strong effects of vestibular input. Other studies also reported that peak coherences do not always align with peak EMG for a range of muscles (Dakin *et al.*, 2013; Forbes *et al.*, 2017; Magnani *et al.*, 2021). Partial alignment between EVS-EMG coupling and muscle activity was demonstrated in the Gastrocnemius muscle where the increase in coherence paralleled the increase in muscle activity but peaked slightly earlier in the gait cycle than the muscle activity (Blouin *et al.*, 2011).

At the lumbar vertebral levels, the difference in EVS-EMG coupling between ipsilateral and contralateral heel strikes might be explained by the functional differences of the two peak activities at these phases of the gait cycle. At lumbar levels, the activations were described as an eccentric contraction at contralateral heel strikes, and a concentric contraction at the ipsilateral heel strikes (Shiavi, 1985; Anders *et al.*, 2007). Our results shows that only the activity at ipsilateral heel strikes

of the lumbar paraspinal muscles was affected by vestibular input, which may signify its role in stabilizing the trunk over the new stance leg.

Vertebral Level Specific Response to EVS

In contrast to the expectation that, given a longer efferent pathway, the response delays would increase from the higher to lower vertebral levels, we found no significant differences in delays between the vertebral levels. This is consistent with a previous study addressing paraspinal muscles from T7 to L4 (Guillaud et al., 2020). However, we found differences in the phases, in which EVS-EMG coherence occurred between vertebral levels. This indicates that the modulation of paraspinal muscles activity based on vestibular afference is different between vertebral levels. This vertebral level specific modulation may reflect differences in vestibulospinal tracts transmitting the signals to motoneurons between vertebral levels (Wilson & Yoshida, 1969; Wilson *et al.*, 1970; Wilson *et al.*, 1995; Kasumacic *et al.*, 2010). Using selective lesions in the brainstem and/or spinal cord in neonatal mice, Kasumacic et al (2010) showed that the vestibular inputs to motoneurons at the upper cervical levels primarily derive from the medial vestibulospinal tracts, while at lower cervical levels, there was a substantial contribution from the lateral vestibulospinal tract. This may potentially explain the constant EVS-EMG coupling at C7 level in our study, which was different from the distinctly phasic responses at the other vertebral levels. The continuous coupling at C7 may be related to head stabilization, an important function of the medial vestibulospinal tracts (Goldberg & Cullen, 2011). At the lumbar levels in mice, vestibular input solely came from the lateral vestibulospinal tracts (Kasumacic *et al.*, 2010). At thoracic levels, early vestibular inputs originated from the lateral vestibulospinal tract, with later inputs potentially transmitted by midline-crossing motoneuron dendrites and/or excitatory commissural interneurons (Kasumacic *et al.*, 2010). Transmission of vestibular signals by different tracts might be expected to cause a difference in response delays. However, the faster conduction velocity (90 m/sec) of the longer lateral-vestibulospinal tract and a slower conduction velocity (60 m/sec) of medial vestibulospinal tract (Peterson *et al.*, 1978) may result in a similar delay and synchronized modulation of paraspinal muscle activity at different vertebral levels as a consequence.

Interestingly, we found that coherent responses at the upper and lower vertebral levels were mirrored, that is to say; at the lower levels, coherence was present around ipsilateral heel strike, while at the higher levels, it was present around contralateral heel strike. From a biomechanical point of view, this spatial pattern of vestibular induced activation could ensure maintenance of head orientation in space, while moving the trunk to correct a deviation of the centre of mass. To be more specific, a left displacement of the centre of mass could be counteracted by the contraction of left lumbar muscles. To maintain the head orientation in space, cervical and upper thorax muscles activity at the right side would be needed. These mirrored responses between upper-ipsilateral and lower-contralateral muscles to the vestibular signals have also been observed in mice (Kasumacic *et al.*, 2010). After ipsilateral hemi-sections of the spinal cord at C1 level in mice, the responses to electrical stimulation in vestibulospinal motoneurons at the contralateral side were completely eliminated at the thoracic and lumbar levels, while at the cervical level the contralateral responses remained unaffected, but disappeared after contralateral hemi-section, and vice versa (Kasumacic *et al.*, 2010). Furthermore, signals from the

ipsilateral-descending lateral vestibulospinal tract are transmitted to contralateral motoneurons by descending commissural interneurons. These interneurons are more prevalent at the T7 level than at L1, L2 and L5 level (Kasumacic *et al.*, 2010; Kasumacic *et al.*, 2015). This finding is in line with our observation that at T5 and T7 levels, the spatial pattern of EVS-EMG coupling resembles a combination of those at higher thoracic and lumbar levels.

Impact of Step Width on Vestibular Contributions

Surprisingly, our outcomes showed no statistically significant differences in EVS-EMG coherence between walking at preferred and narrow step widths. In contrast, in an earlier study, EVS-EMG coherence of the lumbar erector spinae muscle significantly increased when walking with narrower step widths, while in medial gastrocnemius and gluteus medius coherence decreased or remained unchanged, respectively (Magnani *et al.*, 2021). One of the reasons could be that in our study, participants did not fully keep to our instructions of halving step width. Moreover, unlike Magnani et al (2021), we did not ask participants to walk with an upward head tilt of 18 degree. Such a posture maximizes the perception of head roll during EVS (Fitzpatrick & Day, 2004; St George & Fitzpatrick, 2011;). Since we imposed step width by lines projected on the treadmill, it was impossible to keep this head orientation. Finally, our sample size was smaller than that in Magnani et al. (2021) and the trend of an increase in EVS-EMG coherence in narrow step width, which in line with previous research, might suggest a lack of power in the present study.

Limitations

One important limitation of this study is that currently there is no validated method to eliminate the artifacts of electrical stimulation from EMG signals. Although the filtered EMG still contains the timing information of activation in muscles evoked by stimulation (Forbes *et al.*, 2018), it is unclear how appropriate the filtering is. Filtering EMG data to remove the EVS artifacts will inevitably also remove EMG and while information on lower bandwidth changes in muscle force is largely maintained or even enhanced (Potvin & Brown, 2004), information on muscle activation in the frequency range of interest here may be lost due this procedure. In addition, rectification of the EMG signals may cause a nonlinear distortion (Neto & Christou, 2010; McClelland *et al.*, 2014), which may enhance (Ward *et al.*, 2013) or decrease coherence (Neto & Christou, 2010) or create false coherence in a frequency range where there is no input (Neto & Christou, 2010). Still, the application of filtering and rectification is reasonable in view of our primary interest in the modulation of muscle activation and coherence over the gait cycle (Myers *et al.*, 2003; Halliday & Farmer, 2010; van Asseldonk *et al.*, 2014; Jiang *et al.*, 2019). Nevertheless, finding an appropriate method for artifact removal may further strengthen our understanding or the electrical stimulus-response relationship.

Conclusion

We explored how vestibular signals influence paraspinal muscle activity at different vertebral levels in walking with preferred and narrow step width. Significant EVS-EMG coupling was observed at all recorded sites around the ipsilateral and/or contralateral heel strikes. This coupling was vertebral level specific and exhibited a mirrored pattern between the left and right side of the body, as well as between the higher and lower vertebral levels. In other words, at the same vertebral level, the coupling on the left side exhibited a phase shift of half a gait cycle compared to the

right side. Along the vertebral levels, a peak occurred at ipsilateral heel strike at lower levels, while it occurred at the contralateral heel strike at higher levels. We found that the EVS-EMG coupling partially coincided with the peak muscle activity. No significant differences were found in gain and delay between either the vertebral levels or step width conditions. Vertebral level specific modulation of paraspinal muscle activity based on vestibular signals might allow a fast, synchronized, and spatially coordinated response along the trunk during walking.

Reference

Ali AS, Rowen KA & Iles JF. (2003). Vestibular actions on back and lower limb muscles during postural tasks in man. *J Physiol* **546,** 615-624.

Anders C, Wagner H, Puta C, Grassme R, Petrovitch A & Scholle HC. (2007). Trunk muscle activation patterns during walking at different speeds. *J Electromyogr Kinesiol* **17,** 245-252.

Arvin M, Mazaheri M, Hoozemans MJM, Pijnappels M, Burger BJ, Verschueren SMP & van Dieen JH. (2016). Effects of narrow base gait on mediolateral balance control in young and older adults. *J Biomech* **49,** 1264-1267.

Basaldella E, Takeoka A, Sigrist M & Arber S. (2015). Multisensory Signaling Shapes Vestibulo-Motor Circuit Specificity. *Cell* **163,** 301-312.

Blouin JS, Dakin CJ, van den Doel K, Chua R, McFadyen BJ & Inglis JT. (2011). Extracting phase-dependent human vestibular reflexes during locomotion using both time and frequency correlation approaches. *J Appl Physiol (1985)* **111,** 1484-1490.

Bruijn SM, Meijer OG, Beek PJ & van Dieen JH. (2013). Assessing the stability of human locomotion: a review of current measures. *J R Soc Interface* **10,** 20120999.

Bruijn SM & van Dieen JH. (2018). Control of human gait stability through foot placement. *J R Soc Interface* **15**.

Callaghan JP, Patla AE & McGill SM. (1999). Low back three-dimensional joint forces, kinematics, and kinetics during walking. *Clin Biomech (Bristol, Avon)* **14,** 203-216.

Cullen KE. (2012). The vestibular system: multimodal integration and encoding of self-motion for motor control. *Trends Neurosci* **35,** 185-196.

Dakin CJ, Inglis JT, Chua R & Blouin JS. (2013). Muscle-specific modulation of vestibular reflexes with increased locomotor velocity and cadence. *J Neurophysiol* **110,** 86-94.

Dakin CJ, Luu BL, van den Doel K, Inglis JT & Blouin JS. (2010). Frequency-specific modulation of vestibular-evoked sway responses in humans. *J Neurophysiol* **103,** 1048-1056.

Day BL. (1999). Galvanic vestibular stimulation: new uses for an old tool. *J Physiol* **517 (Pt 3),** 631.

de Leva P. (1996). Adjustments to Zatsiorsky-Seluyanov's segment inertia parameters. *J Biomech* **29,** 1223-1230.

de Seze M, Falgairolle M, Viel S, Assaiante C & Cazalets JR. (2008). Sequential activation of axial muscles during different forms of rhythmic behavior in man. *Exp Brain Res* **185,** 237-247.

Dichgans J & Diener HC. (1989). The contribution of vestibulo-spinal mechanisms to the maintenance of human upright posture. *Acta Otolaryngol* **107,** 338-345.

Fitzpatrick RC & Day BL. (2004). Probing the human vestibular system with galvanic stimulation. *J Appl Physiol (1985)* **96,** 2301-2316.

Forbes PA, Dakin CJ, Vardy AN, Happee R, Siegmund GP, Schouten AC & Blouin JS. (2013). Frequency response of vestibular reflexes in neck, back, and lower limb muscles. *J Neurophysiol* **110,** 1869-1881.

Forbes PA, Fice JB, Siegmund GP & Blouin JS. (2018). Electrical Vestibular Stimuli Evoke Robust Muscle Activity in Deep and Superficial Neck Muscles in Humans. *Front Neurol* **9,** 535.

Forbes PA, Kwan A, Rasman BG, Mitchell DE, Cullen KE & Blouin JS. (2020). Neural Mechanisms Underlying High-Frequency Vestibulocollic Reflexes In Humans And Monkeys. *J Neurosci* **40,** 1874-1887.

Forbes PA, Vlutters M, Dakin CJ, van der Kooij H, Blouin JS & Schouten AC. (2017). Rapid limb-specific modulation of vestibular contributions to ankle muscle activity during locomotion. *J Physiol* **595,** 2175-2195.

Fukushima K, Peterson BW & Wilson VJ. (1979). Vestibulospinal, reticulospinal and interstitiospinal pathways in the cat. *Prog Brain Res* **50,** 121-136.

Goldberg JM & Cullen KE. (2011). Vestibular control of the head: possible functions of the vestibulocollic reflex. *Exp Brain Res* **210,** 331-345.

Goldberg JM, Fernandez C & Smith CE. (1982). Responses of vestibular-nerve afferents in the squirrel monkey to externally applied galvanic currents. *Brain Res* **252,** 156-160.

Grillner S & Hongo T. (1972). Vestibulospinal effects on motoneurones and interneurones in the lumbosacral cord. *Prog Brain Res* **37,** 243-262.

Guillaud E, Faure C, Doat E, Bouyer LJ, Guehl D & Cazalets JR. (2020). Ancestral persistence of vestibulospinal reflexes in axial muscles in humans. *J Neurophysiol* **123,** 2010-2023.

Halliday DM & Farmer SF. (2010). On the need for rectification of surface EMG. *J Neurophysiol* **103,** 3547; author reply 3548-3549.

Hof AL. (2007). The equations of motion for a standing human reveal three mechanisms for balance. *J Biomech* **40,** 451-457.

Ivanenko YP, Poppele RE & Lacquaniti F. (2004). Five basic muscle activation patterns account for muscle activity during human locomotion. *J Physiol* **556,** 267-282.

Ivanenko YP, Poppele RE & Lacquaniti F. (2006). Spinal cord maps of spatiotemporal alpha-motoneuron activation in humans walking at different speeds. *J Neurophysiol* **95,** 602-618.

Jiang X, Bian GB & Tian Z. (2019). Removal of Artifacts from EEG Signals: A Review. *Sensors (Basel)* **19**.

Kasumacic N, Glover JC & Perreault MC. (2010). Segmental patterns of vestibular-mediated synaptic inputs to axial and limb motoneurons in the neonatal mouse assessed by optical recording. *J Physiol* **588,** 4905-4925.

Kasumacic N, Lambert FM, Coulon P, Bras H, Vinay L, Perreault MC & Glover JC. (2015). Segmental organization of vestibulospinal inputs to spinal interneurons mediating crossed activation of thoracolumbar motoneurons in the neonatal mouse. *J Neurosci* **35,** 8158-8169.

Kwan A, Forbes PA, Mitchell DE, Blouin JS & Cullen KE. (2019). Neural substrates, dynamics and thresholds of galvanic vestibular stimulation in the behaving primate. *Nat Commun* **10,** 1904.

Magnani RM, Bruijn SM, van Dieen JH & Forbes PA. (2021). Stabilization demands of walking modulate the vestibular contributions to gait. *Sci Rep* **11,** 13736.

Magnani RM, van Dieen JH & Bruijn SM. (2023). Effects of vestibular stimulation on gait stability when walking at different step widths. *Exp Brain Res* **241,** 49-58.

Maris E, Schoffelen JM & Fries P. (2007). Nonparametric statistical testing of coherence differences. *J Neurosci Methods* **163,** 161-175.

Markham CH. (1987). Vestibular control of muscular tone and posture. *Can J Neurol Sci* **14,** 493-496.

Mazaheri M, Coenen P, Parnianpour M, Kiers H & van Dieen JH. (2013). Low back pain and postural sway during quiet standing with and without sensory manipulation: a systematic review. *Gait Posture* **37,** 12-22.

McClelland VM, Cvetkovic Z & Mills KR. (2014). Inconsistent effects of EMG rectification on coherence analysis. *J Physiol* **592,** 249-250.

Murray AJ, Croce K, Belton T, Akay T & Jessell TM. (2018). Balance Control Mediated by Vestibular Circuits Directing Limb Extension or Antagonist Muscle Co-activation. *Cell Rep* **22,** 1325-1338.

Myers LJ, Lowery M, O'Malley M, Vaughan CL, Heneghan C, St Clair Gibson A, Harley YX & Sreenivasan R. (2003). Rectification and non-linear pre-

processing of EMG signals for cortico-muscular analysis. *J Neurosci Methods* **124,** 157-165.

Neto OP & Christou EA. (2010). Rectification of the EMG signal impairs the identification of oscillatory input to the muscle. *J Neurophysiol* **103,** 1093-1103.

Peterson BW, Maunz RA & Fukushima K. (1978). Properties of a new vestibulospinal projection, the caudal vestibulospinal tract. *Exp Brain Res* **32,** 287-292.

Potvin JR & Brown SH. (2004). Less is more: high pass filtering, to remove up to 99% of the surface EMG signal power, improves EMG-based biceps brachii muscle force estimates. *J Electromyogr Kinesiol* **14,** 389-399.

Roerdink M, Coolen BH, Clairbois BH, Lamoth CJ & Beek PJ. (2008). Online gait event detection using a large force platform embedded in a treadmill. *J Biomech* **41,** 2628-2632.

Shiavi R. (1985). Electromyographic patterns in adult locomotion: a comprehensive review. *J Rehabil Res Dev* **22,** 85-98.

Sprenger A, Wojak JF, Jandl NM & Helmchen C. (2017). Postural Control in Bilateral Vestibular Failure: Its Relation to Visual, Proprioceptive, Vestibular, and Cognitive Input. *Front Neurol* **8,** 444.

St George RJ & Fitzpatrick RC. (2011). The sense of self-motion, orientation and balance explored by vestibular stimulation. *J Physiol* **589,** 807-813.

van Asseldonk EH, Campfens SF, Verwer SJ, van Putten MJ & Stegeman DF. (2014). Reliability and agreement of intramuscular coherence in tibialis anterior muscle. *PLoS One* **9,** e88428.

van Schooten KS, Sloot LH, Bruijn SM, Kingma H, Meijer OG, Pijnappels M & van Dieen JH. (2011). Sensitivity of trunk variability and stability measures to balance impairments induced by galvanic vestibular stimulation during gait. *Gait Posture* **33,** 656-660.

Ward NJ, Farmer SF, Berthouze L & Halliday DM. (2013). Rectification of EMG in low force contractions improves detection of motor unit coherence in the beta-frequency band. *J Neurophysiol* **110,** 1744-1750.

Wilson VJ, Boyle R, Fukushima K, Rose PK, Shinoda Y, Sugiuchi Y & Uchino Y. (1995). The vestibulocollic reflex. *J Vestib Res* **5,** 147-170.

Wilson VJ & Maeda M. (1974). Connections between semicircular canals and neck motorneurons in the cat. *J Neurophysiol* **37,** 346-357.

Wilson VJ & Yoshida M. (1969). Comparison of effects of stimulation of Deiters' nucleus and medial longitudinal fasciculus on neck, forelimb, and hindlimb motoneurons. *J Neurophysiol* **32,** 743-758.

Wilson VJ, Yoshida M & Schor RH. (1970). Supraspinal monosynaptic excitation and inhibition of thoracic back montoneurons. *Exp Brain Res* **11,** 282-295.

Zhan Y, Halliday D, Jiang P, Liu X & Feng J. (2006). Detecting time-dependent coherence between non-stationary electrophysiological signals--a combined statistical and time-frequency approach. *J Neurosci Methods* **156,** 322-332.

Funding

Yiyuan C. Li was funded by a scholarship (No. 202108520034) from China Scholarship Council (CSC). Sjoerd M. Bruijn was funded by a VIDI grant (no. 016.Vidi.178.014) from the Dutch Organization for Scientific Research (NWO).